arXiv:1302.4017v1 [cond-mat.mes-hall] 17 Feb 2013

Long-Range Interaction of Spin-Qubits via Ferromagnets

Luka Trifunovic, Fabio L. Pedrocchi, and Daniel Loss
Department of Physics, University of Basel, Klingelbergstrasse 82, CH-4056 Basel, Switzerland
(Dated: February 19, 2013)

We propose a mechanism of long-range coherent coupling between spins coupled to a ferromagnet by exchnage or dipolar coupling. An effective two-spin interaction Hamiltonian is derived and the coupling strength is estimated. We also discuss mechanisms of decoherence and consider possibilities for gate control of the interaction between neighboring spin-qubits. The resulting quantum computing architecture retains all the single qubit gates and measurement aspects of earlier approaches, but allows qubit spacing at distances of order 1 μm for two-qubit gates, achievable with current semiconductor technology. The clock speed depends strongly on the dimensionality of the ferromagnet and is between MHz and GHz.

PACS numbers: 73.20.Dx, 71.70.Ej, 03.67.Lx, 76.60.-k

Introduction. Quantum coherence and entanglement lie at the heart of quantum information processing. One of the basic requirements for implementing quantum computing is to generate, control, and, measure entanglement in a given quantum system. This is a rather challenging task, as it requires to overcome several obstacles, the most important one being decoherence processes. These negative effects have their origin in the unavoidable coupling of the quantum systems to the environment they are residing in.

An unwritten rule in the search for a good system to encode qubits is the smaller the system the more coherence, or, more precisely, the fewer degrees of freedom the weaker the coupling to the environment. Simultaneously, one needs to be able to coherently manipulate the individual quantum objects, which is more efficient for larger systems. This immediately forces us to compromise between manipulation and decoherence requirements.

Following this rule, one of the most successful candidates for encoding a qubit is an electron spin localized in a semiconductor quantum dot, gate-defined or self-assembled [1]. Indeed, this natural two-level system fulfills most of the prerequisites for a good qubit; it is very long-lived (relaxation time $T_1 \sim 1s$ [2] and decoherence time $T_2 \sim 300\mu s$ [3]), it can be controlled efficiently by both electric and magnetic fields [4–6], and, eventually, may be scaled into a large network. However, one of the central challenges for this scaling remains the qubit-qubit coupling, in particular, via distances that give enough space to accommodate gates and control lines that are needed for engineering large networks.

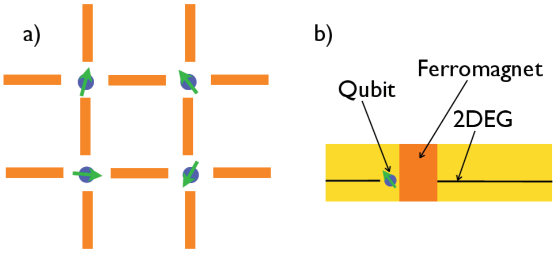

FIG. 1. The schematics of the two-dimensional quantum computer architecture. The left panel (a), shows the top view of the architecture proposed. The orange parts represent ferromagnet, while the blue circles represent localized electron whose spin (green) is used to define a qubit. The right panel (b) depicts the side view of the setup. The ferromagnet can be placed in vicinity of the qubit by etching a trench and thus also removing part of 2DEG (black line).

Addressing this issue, we propose in this work a setup to couple two spin qubits separated by a relatively large distance on the order of micrometers, see Fig. 1a. In contrast to other schemes [7–11], the coupling is mediated via a ferromagnet to which the spin qubits are coupled by exchange or dipolar interaction. The local exchange coupling between the ferromagnet and the spin qubits can be realized by etching a trench close to the spin qubit and placing a ferromagnet therein, see Fig. 1b. Alternatively, the ferromagnet can be placed on top of the qubit structure and coupled to the qubit spin via dipole-dipole interaction. The switching *on* and *off* the qubit-qubit interaction is achieved either by controlling the tunnel coupling to the ferromagnet by electrical means or by tuning qubits off resonance (see below). The resulting system is thus realizable with state-of-the-art semiconductor technologies.

Let us first give an intuitive picture of the qubit-qubit coupling, before we proceed with the quantitative analysis. The coupling between two distant qubits is mediated via a *coupler* system. The relevant quantity of this coupler is its spin-spin susceptibility—in order to have a long-range coupling, a slowly spatially decaying susceptibility is required. Thus, the dimensionality of the coupler plays an important role since, in general, it strongly influences the spatial decay of the susceptibility, which can be anticipated from purely geometric considerations. Furthermore, since we are interested in coherent interactions between the qubits, care must be taken that the coupler does not introduce detrimental decoherence—the quantity containing information about this is the noise power spectrum $S(\omega)$ of the coupler, which, in turn, is related to the imaginary part of the coupler susceptibility via the fluctuation-dissipation theorem.

When the qubits are separated by a distance of $1\mu m$, the coupling strength of qubit-qubit interaction reaches values of 10^{-10}eV for a 3D tunnel coupled ferromagnet. Furthermore, we show that the tunnel and dipolar couplings to ferromagnet do not cause additional decoherence problems since the decoherence times due to it can be tailored to be as long as several minutes. Much better qubit-qubit coupling strengths, on the order of 10^{-6}eV, can be obtained if a quasi-1D ferromagnet (magnetic semiconductor) is used as a coupler. Finally, if the coupling to the ferromagnet is of dipolar origin, a coupling strength of 10^{-8}eV can be reached.

Exchange coupling. We denote by $\boldsymbol{S}_{\mathbf{r}}$ the spins (of size S) of the ferromagnet at site $\mathbf{r}$ on a cubic lattice and $\boldsymbol{\sigma}_i$ stands for the spin-1/2 qubit spins. The Hamiltonian we consider is of the following form

$$H = H_F + H_\sigma + A\sum_{i} \boldsymbol{\sigma}_i \cdot \boldsymbol{S}_{\mathbf{r}_i}\,, \tag{1}$$

where A is the exchange coupling constant between the qubit spins and the ferromagnet (for the dipolar coupling, see below). The Hamiltonian of the ferromagnet, $H_F = -J\sum_{\langle \mathbf{r},\mathbf{r}'\rangle} \boldsymbol{S}_{\mathbf{r}} \cdot \boldsymbol{S}_{\mathbf{r}'}$ with $J > 0$, is the three-dimensional (3D) Heisenberg model with the sum restricted to nearest-neighbor sites $\langle \mathbf{r}, \mathbf{r}'\rangle$. The ferromagnet is assumed to be below the Curie temperature with the magnetization pointing along the z-direction. The qubit Hamiltonian is assumed to be without splitting initially, that is $H_\sigma = 0$. Nevertheless, since the ferromagnet is in the ordered phase, there exists a first order effect due to coupling to the ferromagnet $H_\sigma = A\sum_i \sigma_i^z \langle S^z_{\mathbf{r}_i}\rangle$. As will become clear later, such a splitting is undesirable if one is interested in *coherent* interaction—we remedy this by coupling the spins to another ferromagnet, albeit with anti-parallel magnetization. Since we allow for some misalignment between orientation of the magnetization of the two ferromagnets, the final Hamiltonian for the qubits in the spin space after correctly taking into account the first order corrections due to coupling to the ferromagnet reads

$$H_\sigma = \frac{1}{2}\Delta \sum_i \sigma_i^x\,. \tag{2}$$

The splitting in the x-direction of the qubit (or equivalently along the y-direction) is beneficial since it reduces decoherence due to longitudinal noise of the ferromagnet: The effect of such noise spectrum can significantly influence decoherence times for the case of no splitting of the qubit because the longitudinal noise is gapless.

Coherent coupling. We proceed with the derivation of an effective two-spin interaction Hamiltonian for $A \ll J$ by employing a perturbative Schrieffer-Wolff transformation [12] up to the second order (see Appendix)

$$H_{\text{eff}} = H_\sigma + \frac{A^2}{8}\chi_\perp(\Delta)(2\sigma_1^y\sigma_2^y - \sigma_1^z\sigma_2^x - \sigma_1^x\sigma_2^z)\,, \tag{3}$$

where we introduced the notation $\chi_\perp(\omega) = \chi_\perp(\omega, L)$ ($L = |\mathbf{r}_2 - \mathbf{r}_1|$) and $\chi_\perp(\omega, \mathbf{r})$ is the transverse real space spin susceptibility of the ferromagnet. Note that we have neglected $\chi_\perp^{3\text{D}}(-\Delta)$ and $\chi_\perp^{3\text{D}}(0)$ in comparison to $\chi_\perp^{1\text{D}}(\Delta)$, as well as the longitudinal susceptibility $\chi_\parallel$ since it is smaller by factor of $1/S$ compared to the transverse one (see Appendix). The real space transverse susceptibility of the 3D ferromagnet is given by (see Appendix)

$$\chi_\perp^{3\text{D}}(\omega, \mathbf{r}) = -\frac{S}{D}\frac{e^{-r/l_F}}{r}, \quad \omega < \Delta_F, \tag{4}$$

where Δ_F is the gap induced via applied external magnetic field or due to internal anisotropy of the ferromagnet, $l_F = \sqrt{\frac{D}{\Delta_F - \omega}}$ and $D = 2JS$. In what follows, we assume that the external gap is always larger than the qubit splitting, $\Delta < \Delta_F$, as this ensures that the transverse noise is not contributing to decoherence since transverse noise is related to the vanishing imaginary part of the transverse susceptibility, $\chi_\perp(\omega)'' = 0$ ($\omega < \Delta_F$). The spatial dependence of the effective two spin coupling given by Eq. (4) is of Yukawa type due to presence of the external gap. If we assume a realistic tunnel coupling to the ferromagnet of 100μeV [7], a Curie temperature of 100K and a gap of $\Delta_F = 100\mu$eV, and the qubit splitting close to the resonance $\Delta_F - \Delta = 3 \times 10^{-3}\mu$eV (corresponding to a magnetic field of about $B = 60\mu$T) we obtain for the qubit-qubit coupling strength a value on the order of 10^{-10}eV for a lattice constant of about 4Å. This coupling strength gives rise to the operation times on the order of $5\mu s$—significantly below the relaxation and decoherence times of the spin qubit, $T_1 = 1s$ [2] and $T_2^* = 300\mu s$ [3] respectively. Furthermore, the error threshold—defined as the ratio between the two-qubit gate operation time to the decoherence time—we obtain with such an operation time is about 10^{-2}, which is good enough for implementing the surface code error correction [13].

The dimensionality of the ferromagnet plays an important role—if we assume $10nm$ width of the trench where the ferromagnet is placed, then, for energies below $0.1m$eV, the ferromagnet behaves as quasi one-dimensional (1D). In this case we obtain (see Appendix)

$$\chi_\perp^{1\text{D}}(\omega, r) = -\frac{S}{D}l_F e^{-r/l_F}, \quad \omega < \Delta_F, \tag{5}$$

wherefrom it is evident that at distances $r \lesssim l_F$ the susceptibility of a quasi-1D ferromagnet is practically constant in contrast to the 3D case, where a $1/r$ decay is obtained, see Eq. (4). Additionally, we require $l_F \lesssim D/(AS) = 2J/A$ for the perturbation theory to be valid. Thus, for the same parameters as above, but without the need to tune very close to the resonance (we set herein $\Delta_F - \Delta = 0.5\mu$eV, corresponding to about $B = 5m$T) a coupling strength of 4×10^{-10}eV is obtained.

For 1D case there is yet another rather promising possibility—to use magnetic semiconductors [14]. These materials are characterized by a particularly low Curie temperature of 30K or below [14], and the distance between the ions that are magnetically ordered via RKKY interaction is about $10-100nm$. Such a large lattice constant is very beneficial for the long range coupling—if we take the lattice constant to be $10nm$, the coupling to the ferromagnet $A = 15\mu$eV and the qubit splitting close to resonance ($\Delta_F - \Delta = 0.5\mu$eV, corresponding to about $B = 5m$T), the qubit-qubit coupling becomes of the order of 1μeV. Such a coupling strength in turn leads to an error threshold on the order of 10^{-6}. Therefore, even the standard error correction protocol can be used in this case.

Finally we note that the bottleneck for the operation time is given by the magnon velocity. The typical magnon energy is given by A, and thus the magnon velocity can be estimated as $v_M = \sqrt{JSA}\, a/\hbar$, leading to times of $10ns$ ($1ns$) for magnons to go over distances of $1\mu m$ in ferromagnets (magnetic semiconductors).

Dipolar coupling. The exchange coupling to the ferromagnet that we considered in the previous section is realistic, albeit experimentally challenging. This motivates us to consider a more feasible setup wherein the ferromagnetic coupler is simply placed on top of the spin-qubit structure [8]. Since there is no overlap between the qubit wave function and the ferromagnet spins in this setup, the qubit-ferromagnet coupling is given by dipole-dipole interaction. Thus, the total Hamiltonian reads $H = H_F + H_\sigma + H_I$, where the interaction between the qubit and the ferromagnet spin, H_I, reads

$$H_I = \sum_{i,\mathbf{r}} \frac{\mu_0 \mu_B \mu}{4\pi r^3} \left(\boldsymbol{\sigma}_i \cdot \boldsymbol{S}_\mathbf{r} - \frac{3(\boldsymbol{\sigma}_i \cdot \mathbf{r})(\boldsymbol{S}_\mathbf{r} \cdot \mathbf{r})}{r^2} \right), \qquad (6)$$

where μ is the magnetic moment of the ferromagnet spins. In order to obtain a sizable coupling and also to simplify the analysis we assume a 'dogbone' shape of the ferromagnetic coupler as in Ref. 8—two ferromagnetic discs connected via a quasi-1D ferromagnetic line. After performing a SW transformation we obtain the effective Hamiltonian

$$H_{\text{eff}} = H_\sigma + \frac{B^2}{32} \chi_\perp^{\text{1D}}(\Delta, L)(2\sigma_1^y \sigma_2^y - \sigma_1^z \sigma_2^x - \sigma_1^x \sigma_2^z)\,, \quad (7)$$

where again we retained only the on-resonance susceptibility, *i.e.*, we neglected $\chi_\perp^{\text{1D}}(-\Delta)$ and $\chi_\perp^{\text{1D}}(0)$ in comparison to $\chi_\perp^{\text{1D}}(\Delta)$. Here, B is given by (see Appendix)

$$B = \frac{\mu_0 \mu_B \mu}{2a^3} \left(\frac{d_2}{\sqrt{d_2^2 + R_0^2}} - \frac{d_1}{\sqrt{d_1^2 + R_0^2}} \right), \qquad (8)$$

where $d_2 - d_1$ is the thickness of the discs, d_1 is the distance in z-direction from the qubit spin to the bottom of the adjacent disc, and R_0 is the disc radius. If we use the same parameters as before for the quasi-1D ferromagnet with lattice constant of 4Å and $\Delta_F - \Delta = 10^{-2}\mu$eV—a coupling strength of 10^{-8}eV is obtained. Here, we assumed $\mu = 10\mu_B$, $d_1 = 50nm$, $d_2 - d_1 = 20nm$, and $R_0 = 50nm$.

The qubit-qubit interaction in case of the dipolar coupling to the ferromagnet can be efficiently switched on (off) by tunning the qubits on- (off-) resonance. Indeed, the susceptibility depends sensitively on the difference $\Delta_F - \Delta$, see Eq. (5), it is enough to detune by less than 1% to practically switch off the coupling. This detuning can be for example achieved by changing the qubit splitting by a spatially dependent g-factor which can be controlled by electrical means. Such a switching scheme will not decouple the ferromagnet as a source of decoherence. Nevertheless, as we will demonstrate below, when the transverse noise is gapped the decoherence caused by the ferromagnet becomes negligible, and thus there is no need to decouple the qubit from the ferromagnet during the *off* state.

Two-qubit gates. Since the Hamiltonian of Eq. (3) is entangling, it can be used to implement two-qubit gates. Here we consider the iSWAP, CPF, and CNOT gates, the last one being widely used in schemes for quantum computation [15]. The Hamiltonian for two single-QD qubits interacting via the ferromagnet is the sum of the qubit-qubit interaction and the Zeeman terms, given in Eq. (3). The strength of the latter in comparison to the former allows us to approximate the Hamiltonian (see Appendix)

$$H'_{\text{eff}} = J_{12}(\sigma_1^y \sigma_2^y + \sigma_1^z \sigma_2^z) + H_\sigma\,, \qquad (9)$$

with the notation $J_{12} = A^2 \chi_\perp(\Delta)/4$ and H_σ given by Eq. (2). After this approximation, the qubit-qubit interaction and Zeeman terms commute. The iSWAP gate, U_{iSWAP}, may then be realized with the following sequence

$$U_{\text{iSWAP}} = \mathcal{H}_1 \mathcal{H}_2 e^{iH_\sigma t} e^{-iH'_{\text{eff}} t} \mathcal{H}_1 \mathcal{H}_2\,, \qquad (10)$$

where $t = 3\pi/(4J_{12})$ and $\mathcal{H}$ denotes the single-qubit Hadamard rotation. More details on the construction can be found in the Appendix. Previously, the sequence for the universal CPF gate was constructed [16] for the same Hamiltonian as the projected one given in Eq. (9), albeit without the Zeeman terms which commute with the Hamiltonian. With the iSWAP the CNOT gate can be constructed in a standard way [17]

$$U_{\text{CNOT}} = e^{-i\frac{\pi}{4}\sigma_1^z} e^{i\frac{\pi}{4}\sigma_2^x} e^{i\frac{\pi}{4}\sigma_2^z} U_{\text{iSWAP}} e^{-i\frac{\pi}{4}\sigma_1^x} U_{\text{iSWAP}} e^{i\frac{\pi}{4}\sigma_2^z}\,. \qquad (11)$$

Since H'_{eff} is only an approximation of the total Hamiltonian, these sequences will yield approximate iSWAP and CNOT. Their success can be characterized by the fidelity, as defined in the Appendix. For realistic parameters, with the Zeeman terms two order of magnitude stronger than the qubit-qubit coupling, the above sequence yields fidelities for the CNOT gate of 99.976%. This is well above the fidelity of 99.17%, corresponding to the threshold for noisy CNOTs in the surface code [18].

Decoherence. Next, we study the dynamics of a single spin qubit coupled to the ferromagnet, but neglecting correlated noise (see Appendix). The qubit dynamics can be described by the reduced density matrix $\rho_{\rm R}(t) = {\rm tr}\,(\rho(t))$, where ρ is the density matrix for the total system and the trace is taken over the ferromagnet. Here, $\rho_{\rm R}(t)$ satisfies the equation [19]

$$\dot{\rho}_{\rm R} = -i[H_\sigma, \rho_{\rm R}] + \mathcal{D}\rho_{\rm R}\,, \tag{12}$$

with $\mathcal{D}$ given by the following expression in the Born-Markov approximation

$$\begin{aligned}\mathcal{D}\rho_{\rm R}(t) =& -A^2 S_\parallel(\Delta)\Big(\rho_{\rm R}(t) - \sigma_p^z\rho_{\rm R}(t)\sigma_p^z\Big) + \\ &+ A^2 C''_\parallel(\Delta)\left([\sigma_p^x, \rho_R]_+ - i\sigma_p^y\rho_R\sigma_p^z + i\sigma_p^z\rho_R\sigma_p^y\right)\,,\end{aligned} \tag{13}$$

where $S_\parallel(\omega)$ is longitudinal noise power of the ferromagnet, defined as Fourier transform of $S_\parallel(t) = \langle[S^z(t), S^z(0)]_+\rangle$, while $C''_\parallel(\omega)$ is defined as imaginary part of the correlation function $C_\parallel(\omega) = \int_0^\infty dt\sin(\omega t)\langle S^z(t)S^z(0)\rangle = \int_0^\infty dt\sin(\omega t)C_\parallel(t)$. In writing Eq. (13) we assumed that the external gap of the ferromagnet, Δ_F, is bigger than the splitting of the qubit (i.e. $\Delta < \Delta_F$). Therefore, the transverse noise of the ferromagnet is not entering in the Born approximation since it is gapped. The 3D ferromagnet behaves as subohmic bath $J_\parallel(\omega) = \tilde{\omega}_s\left(\frac{\omega}{\omega_s}\right)^s$ with $s = 1/2$, $\omega_s = T$ and $\tilde{\omega}_s = \alpha T^2/D^3 e^{-\beta\Delta_F}$, where $\alpha = \frac{\sqrt{\pi}-e\pi{\rm Erfc}(1)}{2} = 0.21$ (see Appendix). From Eq. (12) we obtain the relaxation and decoherence times [19] for the 3D ferromagnet under the assumption $\Delta_F \gg T$

$$T_1^{-1} = A^2 S_\parallel^{\rm 3D}(\Delta) = \frac{\alpha A^2\sqrt{\beta\Delta}}{2\beta^2 D^3}e^{-\beta\Delta_F}\coth(\beta\Delta/2). \tag{14}$$

The decoherence time becomes $T_2 = 2\,T_1$. The above formula allows us to estimate the additional decoherence and relaxation due to the ferromagnet. If we assume temperatures below 0.1K, we get decoherence times due to ferromagnet of about an hour. Such a long decoherence time is obtained mainly because we choose parameters in such a way that the transverse susceptibility is gapped. The remaining longitudinal noise of the ferromagnet vanishes at zero temperature and by choosing reasonably low temperatures (compared to Δ_F) this noise source can be significantly reduced. Furthermore, for quasi-1D ferromagnets, we obtain divergent (as $\omega \to 0$) spectral density with $s = -1/2$, $\omega_s = T$ and $\tilde{\omega}_s = \frac{\gamma}{D}e^{-\beta\Delta_F}$. The relaxation rate is now given by

$$T_1^{-1} = A^2 S_\parallel^{\rm 1D}(\Delta) = \frac{\gamma A^2}{D\sqrt{\beta\Delta}}e^{-\beta\Delta_F}\coth(\beta\Delta/2)\,, \tag{15}$$

where γ is a numerical factor of order 1. As before, the decoherence time reads $T_2 = 2\,T_1$. With the same temperature and the external gap as for the 3D case, the decoherence time is about milliseconds.

Similarly, the relaxation time for dipolar coupling reads

$$\begin{aligned}T_1^{-1} =& \frac{\mu_0^2\mu_B^2\mu^2}{2a^6}\int_{\rm disc}\frac{d\mathbf{r}'d\mathbf{r}''}{r'^3 r''^3}\left(1-\frac{3z'^2}{r'^2}\right)\left(1-\frac{3z''^2}{r''^2}\right)\times \\ &\times S_\parallel(\Delta, \mathbf{r}''-\mathbf{r}').\end{aligned} \tag{16}$$

Instead of explicitly calculating the above integral we can readily give a lower bound for the relaxation (and decoherence) time using a rather general inequality, $S_\parallel$. Thus the lower bound for the relaxation time is given

$$T_1^{-1} \leq B^2 S_\parallel^{\rm 3D}(\Delta), \tag{17}$$

where B is given in Eq. (8) and $S_\parallel^{\rm 3D}(\Delta)$ in Eq. (14). This leads to the lower bound of the relaxation time which is on the order of minutes.

We note that the effect of the noise is, by and large, more pronounced for $\Delta = 0$ and this was the main motivation for us to introduce $\Delta \neq 0$. In order to clarify the behavior of the system when $\Delta = 0$, we study in the Appendix an exactly solvable model which demonstrates the limitation of the Born approximation.

Conclusions. The clock speed of the quantum computer architecture just described appears to be a fraction of MHz (3D ferromagnet) and 1GHz (quasi 1D magnetic semiconductor) and should be compared with the time scales for relaxation and decoherence. The leading mechanism for these at low temperatures is through interaction with nuclear spins for, say, spin qubits in GaAs dots. Typically, the decoherence time T_2^* is of order 300μs [3]. In our case, there is no significant additional decoherence mechanisms caused by tunnel or dipolar coupling to the ferromagnet.

The standard quantum error correction protocols require the quality factor, equal the ratio of the gate-function clock time to decoherence time, not to exceed 10^{-5}. Our estimates indicate that this is not the case for the present system when a 3D ferromagnet is used. However, there exist error correction schemes with significantly higher error threshold, such as surface code with error threshold of 10^{-2} [13]. Since the architecture proposed herein satisfies all the criteria for implementing the surface code error correction, we conclude that our proposal satisfies the criteria for scalability of a quantum computer. Additionally, when quasi-1D magnetic semiconductors are used as couplers, even the standard quantum error correction protocols can be used.

Acknowledgements. We would like to thank A. Yacoby for useful discussions. This work was supported by SNF, NCCR QSIT, and IARPA.

[1] C. Kloeffel and D. Loss, ArXiv e-prints (2012), arXiv:1204.5917.

[2] S. Amasha, K. MacLean, I. P. Radu, D. M. Zumbühl, M. A. Kastner, M. P. Hanson, and A. C. Gossard, Phys. Rev. Lett. **100**, 046803 (2008).

[3] H. Bluhm, S. Foletti, I. Neder, M. Rudner, D. Mahalu, V. Umansky, and A. Yacoby, Nat Phys **7**, 109 (2011).

[4] J. R. Petta, A. C. Johnson, J. M. Taylor, E. A. Laird, A. Yacoby, M. D. Lukin, C. M. Marcus, M. P. Hanson, and A. C. Gossard, Science **309**, 2180 (2005).

[5] F. H. L. Koppens, K. C. Nowack, and L. M. K. Vandersypen, Phys. Rev. Lett. **100**, 236802 (2008).

[6] R. Brunner, Y.-S. Shin, T. Obata, M. Pioro-Ladrière, T. Kubo, K. Yoshida, T. Taniyama, Y. Tokura, and S. Tarucha, Phys. Rev. Lett. **107**, 146801 (2011).

[7] D. Loss and D. P. DiVincenzo, Phys. Rev. A **57**, 120 (1998).

[8] L. Trifunovic, O. Dial, M. Trif, J. R. Wootton, R. Abebe, A. Yacoby, and D. Loss, Phys. Rev. X **2**, 011006 (2012).

[9] M. D. Shulman, O. E. Dial, S. P. Harvey, H. Bluhm, V. Umansky, and A. Yacoby, Science **336**, 202 (2012).

[10] L. Childress, A. S. Sørensen, and M. D. Lukin, Phys. Rev. A **69**, 042302 (2004).

[11] M. Trif, V. N. Golovach, and D. Loss, Phys. Rev. B **77**, 045434 (2008).

[12] S. Bravyi, D. DiVincenzo, and D. Loss, Ann. Phys. **326**, 2793 (2011).

[13] R. Raussendorf and J. Harrington, Phys. Rev. Lett. **98**, 190504 (2007).

[14] H. Ohno, D. Chiba, F. Matsukura, T. Omiya, E. Abe, T. Dietl, Y. Ohno, and K. Ohtani, Nature **408**, 944 (2000).

[15] M. A. Nielsen and I. L. Chuang, *Quantum Computation and Quantum Information*, 1st ed. (Cambridge University Press, 2004).

[16] A. Imamoglu, D. D. Awschalom, G. Burkard, D. P. DiVincenzo, D. Loss, M. Sherwin, and A. Small, Phys. Rev. Lett. **83**, 4204 (1999).

[17] T. Tanamoto, K. Maruyama, Y. X. Liu, X. Hu, and F. Nori, Phys. Rev. A **78**, 062313 (2008).

[18] D. S. Wang, A. G. Fowler, and L. C. L. Hollenberg, Phys. Rev. A **83**, 020302 (2011).

[19] D. P. DiVincenzo and D. Loss, Phys. Rev. B **71**, 035318 (2005).

arXiv:1302.4017v1 [cond-mat.mes-hall] 17 Feb 2013

Supplementary Material to “Indirect Interaction of Spins via Ferromagnet”

Luka Trifunovic, Fabio L. Pedrocchi, and Daniel Loss
Department of Physics, University of Basel, Klingelbergstrasse 82, CH-4056 Basel, Switzerland

HOLSTEIN-PRIMAKOFF TRANSFORMATION

For the sake of completeness we derive in this Appendix explicit expressions for the different spin-spin correlators used in this work

$$C^{\alpha\beta}(\omega,\mathbf{q}) = \langle S^{\alpha}_{\mathbf{q}}(\omega) S^{\beta}_{-\mathbf{q}}(0)\rangle\,. \tag{1}$$

For this purpose, we make use of a Holstein-Primakoff transformation

$$S_i^z = -S + n_i,\ \ S_i^- = \sqrt{2S}\sqrt{1-\frac{n_i}{2S}}a_i,\ \text{ and}$$
$$S_i^+ = \left(S_i^-\right)^\dagger\,, \tag{2}$$

in the limit $n_i \ll 2S$, with a_i satisfying bosonic commutation relations and $n_i = a_i^\dagger a_i$ [1]. The creation operators $a_i^\dagger$ and annihilation operators a_i satisfy bosonic commutation relations and the associated particles are called magnons. The corresponding Fourier transforms are straightforwardly defined as $a^\dagger_{\mathbf{q}} = \frac{1}{\sqrt{N}}\sum_i e^{-i\mathbf{q}\cdot\mathbf{R}_i} a_i$. In harmonic approximation, the Heisenberg Hamiltonian H_F reads

$$H_F \approx \sum_{\mathbf{q}} \epsilon_{\mathbf{q}} a^\dagger_{\mathbf{q}} a_{\mathbf{q}}\,, \tag{3}$$

where $\epsilon_{\mathbf{q}} = \omega_{\mathbf{q}} + \Delta_F = 4JS[3-(\cos(q_x)+\cos(q_y)+\cos(q_z))] + \Delta_F$ is the spectrum for a cubic lattice with lattice constant $a=1$ and the gap Δ_F is induced by the external magnetic field or anisotropy of the ferromagnet.

TRANSVERSE CORRELATORS $\langle S^+_{\mathbf{q}}(t) S^-_{-\mathbf{q}}(0)\rangle$

Let us now define the Fourier transforms in the harmonic approximation

$$S^+_{\mathbf{q}} = \frac{1}{\sqrt{N}}\sum_i e^{-i\mathbf{q}\mathbf{r}_i} S_i^+ = \frac{\sqrt{2S}}{\sqrt{N}}\sum_i e^{-i\mathbf{q}\mathbf{r}_i} a_i^\dagger = \sqrt{2S} a^\dagger_{-\mathbf{q}}\,,$$
$$S^-_{-\mathbf{q}} = \frac{1}{\sqrt{N}}\sum_i e^{i\mathbf{q}\mathbf{r}_i} S_i^- = \frac{\sqrt{2S}}{\sqrt{N}}\sum_i e^{i\mathbf{q}\mathbf{r}_i} a_i = \sqrt{2S} a_{-\mathbf{q}}\,. \tag{4}$$

From this it directly follows that

$$\begin{aligned} C^{+-}(t,\mathbf{q}) &= \langle S^+_{\mathbf{q}}(t) S^-_{-\mathbf{q}}(0)\rangle \\ &= 2S\langle a^\dagger_{-\mathbf{q}}(t) a_{-\mathbf{q}}\rangle = 2S e^{i\epsilon_{\mathbf{q}} t} n_{\mathbf{q}}\,, \end{aligned} \tag{5}$$

with $\epsilon_{\mathbf{q}} \approx D\mathbf{q}^2 + \Delta_F$ in the harmonic approximation.

The Fourier transform is then simply given by

$$\begin{aligned} C^{+-}(\omega,\mathbf{q}) &= \frac{1}{\sqrt{2\pi}}\int_{-\infty}^{\infty} dt e^{-i\omega t} C^{+-}(t,\mathbf{q}) \\ &= \underbrace{\frac{1}{\sqrt{2\pi}}\int_{-\infty}^{\infty} dt e^{i(\epsilon_{\mathbf{q}}-\omega)t}}_{\sqrt{2\pi}\delta(\epsilon_{\mathbf{q}}-\omega)} 2S n_{\mathbf{q}} \\ &= \sqrt{2\pi} 2S\delta(\epsilon_{\mathbf{q}}-\omega)\frac{1}{e^{\beta\omega}-1}\,. \end{aligned} \tag{6}$$

The corresponding correlator in real space is then simply given by ($q := |\mathbf{q}|$)

$$\begin{aligned} C^{+-}(\omega,\mathbf{r}) &= \frac{1}{(2\pi)^{3/2}}\int d\mathbf{q} e^{i\mathbf{q}\mathbf{r}} C^{+-}(\omega,\mathbf{q}) \\ &= \frac{\sqrt{2\pi}}{(2\pi)^{3/2}} 2S\frac{1}{e^{\beta\omega}-1}\int d\mathbf{q}\delta(D\mathbf{q}^2+\Delta_F-\omega) e^{i\mathbf{q}\mathbf{r}} \\ &= \frac{2S}{e^{\beta\omega}-1}\int_{-1}^{1}\int_0^\infty dq dx q^2\delta(Dq^2+\Delta_F-\omega) e^{iqrx} \\ &= \frac{4S}{r}\frac{1}{e^{\beta\omega}-1}\int_0^\infty dq q\delta(Dq^2+\Delta_F-\omega)\sin(qr)\,. \end{aligned} \tag{7}$$

Let us now perform the following substitution

$$y = Dq^2, \tag{8}$$

which gives for $\omega > \Delta_F$

$$\begin{aligned} C^{+-}(\omega,\mathbf{r}) &= \frac{4S/r}{2D(e^{\beta\omega}-1)}\int_0^\infty dy\delta(y+\Delta_F-\omega)\times \\ &\quad\times\sin\left(\sqrt{\frac{y}{D}}r\right) \\ &= \frac{2S}{D}\frac{1}{e^{\beta\omega}-1}\frac{\sin(\sqrt{(\omega-\Delta_F)/D}r)}{r}\,. \end{aligned} \tag{9}$$

We remark that

$$C^{+-}(\omega,\mathbf{r}) = 0,\quad \omega < \Delta_F. \tag{10}$$

We note the diverging behavior of the above correlation function for $\Delta_F = 0$ and $\omega\to 0$, namely

$$\begin{aligned} \lim_{\omega\to 0}\frac{1}{e^{\beta\omega}-1}\frac{\sin\left(\sqrt{\frac{\omega}{D}}r\right)}{r} &= \lim_{\omega\to 0}\frac{\sqrt{\omega/D}r}{r\beta\omega} \\ &\to \frac{1}{\sqrt{D}\beta}\frac{1}{\sqrt{\omega}}\,. \end{aligned} \tag{11}$$

Similarly, it is now easy to calculate the corresponding commutators and anticommutators. Let us define

$$S_\perp(t,\mathbf{q}) := \frac{1}{2}\{S^+_{\mathbf{q}}(t), S^-_{-\mathbf{q}}(0)\}\,. \tag{12}$$

It is then straightforward to show that

$$S_\perp(t,\mathbf{q}) = S e^{i\epsilon_{\mathbf{q}} t}(1+2n_{\mathbf{q}})\,, \tag{13}$$

and therefore

$$\begin{aligned} S_\perp(\omega,\mathbf{q}) &= \frac{S}{\sqrt{2\pi}}\int_{-\infty}^{\infty} e^{i(\epsilon_{\mathbf{q}}-\omega)t}(1+2n_{\mathbf{q}}) \\ &= S\sqrt{2\pi}\delta(\epsilon_{\mathbf{q}}-\omega)\left(1+2\frac{1}{e^{\beta\omega}-1}\right). \end{aligned} \tag{14}$$

Following essentially the same steps as the one performed above, we obtain the 3D real space anticommutator for $\omega > \Delta_F$

$$\begin{aligned} S_\perp^{3\mathrm{D}}(\omega,\mathbf{q}) &= S\coth(\beta\omega/2)\times \qquad (15)\\ &\times \int_{-1}^{1}\int_{0}^{\infty} dxdqq^2 e^{iqrx}\delta(\epsilon_{\mathbf{q}}-\omega) \\ &= \frac{S}{D}\coth(\beta\omega/2)\frac{\sin(\sqrt{(\omega-\Delta_F)/D}r)}{r}\,. \qquad (16) \end{aligned}$$

Let us now finally calculate the transverse susceptibility defined as

$$\chi_\perp(t,\mathbf{q}) = -i\theta(t)[S^+_{\mathbf{q}}(t), S^-_{-\mathbf{q}}(0)]\,. \tag{17}$$

As before, in the harmonic approximation, one finds

$$\chi_\perp(t,\mathbf{q}) = i\theta(t)2Se^{i\epsilon_{\mathbf{q}}t}\,. \tag{18}$$

In the frequency domain, we then have

$$\begin{aligned} \chi_\perp(\omega,\mathbf{q}) &= \frac{2iS}{\sqrt{2\pi}}\int_0^\infty dte^{i(\epsilon_{\mathbf{q}}-\omega)t-\eta t} \\ &= -\frac{2S}{\sqrt{2\pi}}\frac{1}{\epsilon_{\mathbf{q}}-\omega+i\eta}\,, \end{aligned} \tag{19}$$

and thus in the small $\mathbf{q}$ expansion

$$\chi_\perp(\omega,\mathbf{q}) = -\frac{2S}{\sqrt{2\pi}}\frac{1}{D\mathbf{q}^2+\Delta_F-\omega+i\eta}\,. \tag{20}$$

In real space, for the three-dimensional case, we obtain

$$\begin{aligned} \chi_\perp^{3\mathrm{D}}(\omega,\mathbf{r}) &= -\frac{2S}{\sqrt{2\pi}}\frac{2\pi}{(2\pi)^{3/2}}\int_0^\infty\int_{-1}^{1} dxdqq^2\frac{1}{D\mathbf{q}^2+\Delta_F-\omega+i\eta}e^{iqrx} \\ &= -\frac{4S}{\sqrt{2\pi}}\frac{2\pi}{(2\pi)^{3/2}}\frac{1}{r}\int_0^\infty dqq\frac{1}{Dq^2+\Delta_F-\omega+i\eta}\sin(qr)\,. \end{aligned} \tag{21}$$

Making use of the Plemelj formula we obtain for $\omega > \Delta_F$

$$\begin{aligned} \chi_\perp^{3\mathrm{D}}(\omega,\mathbf{r}) &= -\frac{2S}{\sqrt{2\pi}}\frac{2\pi}{(2\pi)^{3/2}}\frac{1}{r}\int_{-\infty}^\infty dqq\frac{1}{Dq^2+\Delta_F-\omega+i\eta}\sin(qr) \\ &= -\frac{2S}{\sqrt{2\pi}}\frac{2\pi}{(2\pi)^{3/2}}\frac{1}{r}P\int_{-\infty}^\infty dq\frac{q}{Dq^2+\Delta_F-\omega}\sin(qr) + i\frac{2S}{\sqrt{2\pi}}\frac{2\pi^2}{(2\pi)^{3/2}}\frac{1}{r}\int_{-\infty}^\infty dqq\delta(Dq^2+\Delta_F-\omega)\sin(qr) \\ &= -\frac{S}{D}\frac{\cos(r\sqrt{(\omega-\Delta_F)/D})}{r} + i\frac{S}{2D}\frac{\sin(\sqrt{(\omega-\Delta_F)/D}r)}{r}\,. \end{aligned} \tag{22}$$

It is worth pointing out that the imaginary part of the susceptibility vanishes

$$\chi_\perp^{3\mathrm{D}}(\omega,\mathbf{r})'' = 0, \quad \omega < \Delta_F, \tag{23}$$

and therefore the susceptibility is purely real and takes the form of a Yukawa potential

$$\chi_\perp^{3\mathrm{D}}(\omega,\mathbf{r}) = -\frac{S}{D}\frac{e^{-r/l_F}}{r}, \quad \omega < \Delta_F, \tag{24}$$

where $l_F = \sqrt{\frac{D}{\Delta_F-\omega}}$.

Note also that the imaginary part of the transverse susceptibility satisfies the well-know fluctuation dissipation theorem

$$S_\perp^{3\mathrm{D}}(\omega,\mathbf{r}) = \coth(\beta\omega/2)\chi_\perp^{3\mathrm{D}}(\omega,\mathbf{r})''\,. \tag{25}$$

In three-dimension the susceptibility decay as $1/r$, where r is measured in lattice constants. For distances of order of $1\mu m$ this leads to four orders of magnitude reduction.

For quasi one-dimensional ferromagnets such a reduction is absent and the transverse susceptibility reads

$$\chi_\perp^{1\mathrm{D}}(\omega,r) = -\frac{S}{D} l_F e^{-r/l_F}, \quad \omega < \Delta_F, \tag{26}$$

where l_F is defined as above and the imaginary part vanishes as above, i.e.,

$$\chi_\perp^{1\mathrm{D}}(\omega,r)'' = 0, \quad \omega < \Delta_F. \tag{27}$$

Similarly for $\omega > \Delta_F$ we have

$$\chi_\perp^{1\mathrm{D}}(\omega,r) = S \frac{\sin\left(\sqrt{(\omega-\Delta_F)/D}r\right)}{\sqrt{D(\omega-\Delta_F)}}, \tag{28}$$

and

$$\chi_\perp^{1\mathrm{D}}(\omega,r)'' = \frac{S}{2D}\sqrt{\frac{D}{\omega-\Delta_F}} \cos\left(\sqrt{(\omega-\Delta_F)/D}r\right). \tag{29}$$

LONGITUDINAL CORRELATORS $\langle S_{\mathbf{q}}^z(t) S_{-\mathbf{q}}^z(0)\rangle$

The longitudinal susceptibility reads

$$\begin{aligned}\chi_\parallel(t,\mathbf{q}) &= -i\theta(t)[S_{\mathbf{q}}^z(t), S_{-\mathbf{q}}^z(0)] \\ &= -\theta(t)\frac{1}{N}\sum_{\mathbf{q}',\mathbf{q}''} e^{it(\epsilon_{\mathbf{q}'}-\epsilon_{\mathbf{q}'+\mathbf{q}})}\langle[a_{\mathbf{q}'}^\dagger a_{\mathbf{q}'+\mathbf{q}}, a_{\mathbf{q}''}^\dagger a_{\mathbf{q}''-\mathbf{q}}]\rangle.\end{aligned} \tag{30}$$

Applying Wick's theorem and performing a Fourier transform, we obtain the susceptibility in frequency domain

$$\chi_\parallel(\omega,\mathbf{q}) = -\frac{1}{N}\sum_{\mathbf{k}} \frac{n_{\mathbf{k}} - n_{\mathbf{k}+\mathbf{q}}}{\omega - \epsilon_{\mathbf{k}+\mathbf{q}} + \epsilon_{\mathbf{k}} + i\eta}, \tag{31}$$

where $n_{\mathbf{k}}$ is the magnons occupation number, which is given by the Bose-Einstein distribution

$$n_k = \frac{1}{e^{\beta\epsilon_{\mathbf{k}}} - 1}, \tag{32}$$

where $\epsilon_{\mathbf{k}}$ is again the magnon spectrum ($\epsilon_{\mathbf{k}} = \omega_{\mathbf{k}} + \Delta_F \approx D\mathbf{k}^2 + \Delta_F$ for small k). Note that the longitudinal susceptibility is proportional to $1/S$, due to the fact that $\epsilon_{\mathbf{k}} - \epsilon_{\mathbf{k}+\mathbf{q}} = \omega_{\mathbf{k}} - \omega_{\mathbf{k}+\mathbf{q}} \propto S$.

Since we are interested in the decoherence processes caused by the longitudinal fluctuations, we calculate the imaginary part of $\chi_\parallel(\omega,\mathbf{q})$ which is related to the fluctuations via the *fluctuation-dissipation theorem*. Performing a small $\mathbf{q}$ expansion and assuming without loss of generality $\omega > 0$, we obtain

$$\begin{aligned}\chi_\parallel^{3\mathrm{D}}(\omega,\mathbf{q})'' &= \frac{\pi}{(2\pi)^3}\int d\mathbf{k}(n_{\mathbf{k}} - n_{\mathbf{k}+\mathbf{q}})\delta(\omega_{\mathbf{k}} - \omega_{\mathbf{k}+\mathbf{q}} + \omega) \\ &= \frac{1}{4\pi}\int_0^\infty dk k^2 \int_{-1}^1 dx \left(\frac{1}{e^{\beta(\Delta_F + Dk^2)} - 1} - \frac{1}{e^{\beta(\omega+\Delta_F+Dk^2)} - 1}\right)\delta(\omega - Dq^2 - 2Dkqx) \\ &= \frac{1}{4\pi}\int_0^\infty dk k^2 \int_{-1}^1 dx \left(\frac{1}{e^{\beta(\Delta_F + Dk^2)} - 1} - \frac{1}{e^{\beta(\omega+\Delta_F+Dk^2)} - 1}\right)\delta\left(k - \frac{\omega - Dq^2}{2Dqx}\right)\left|\frac{1}{2Dqx}\right| \\ &= \frac{1}{4\pi}\int_{-1}^1 dx \left|\frac{1}{2Dqx}\right| \left(\frac{\omega - Dq^2}{2Dqx}\right)^2 \left(\frac{1}{e^{\beta\left(\Delta_F + D\left(\frac{\omega-Dq^2}{2Dqx}\right)^2\right)} - 1} - \frac{1}{e^{\beta\left(\omega+\Delta_F + D\left(\frac{\omega-Dq^2}{2Dqx}\right)^2\right)} - 1}\right)\theta\left(\frac{\omega - Dq^2}{2Dqx}\right) \\ &= \frac{1}{4\pi}\int_0^1 dx \frac{1}{2Dqx}\left(\frac{\omega - Dq^2}{2Dqx}\right)^2 \left(\frac{1}{e^{\beta\left(\Delta_F + D\left(\frac{\omega-Dq^2}{2Dqx}\right)^2\right)} - 1} - \frac{1}{e^{\beta\left(\omega+\Delta_F + D\left(\frac{\omega-Dq^2}{2Dqx}\right)^2\right)} - 1}\right).\end{aligned} \tag{33}$$

Next, since we are interested in the regime where $\omega \gg T$ (and thus $\beta\omega \gg 1$), we have $n_{\boldsymbol{k}} \gg n_{\boldsymbol{k}+\boldsymbol{q}}$. Furthermore, we approximate the distribution function $n_{\boldsymbol{k}} = \frac{e^{-\beta(\Delta_F + \omega_{\boldsymbol{k}})}}{1 - e^{-\beta\Delta_F} + \beta\omega_{\boldsymbol{k}}}$ (this is valid when $\beta\omega_{\mathbf{k}} \ll 1$) and arrive at the following expression

$$\chi_{\|}^{\mathrm{3D}}(\omega,\mathbf{q})'' = \frac{1}{4\pi}\int_0^1 dx \frac{1}{2Dqx}\left(\frac{\omega - Dq^2}{2Dqx}\right)^2 \frac{e^{-\beta\left(\Delta_F + D\left(\frac{\omega-Dq^2}{2Dqx}\right)^2\right)}}{1 - e^{-\beta\Delta_F} + \beta D\left(\frac{\omega-Dq^2}{2Dqx}\right)^2}$$
$$= -\frac{e^{1-e^{-\beta\Delta_F}-\beta\Delta_F}}{4\beta D^2 q}\mathrm{Ei}\left(e^{-\beta\Delta_F} + \frac{1}{4}\left(-4 - \beta Dq^2 + 2\beta\omega - \frac{\beta\omega^2}{Dq^2}\right)\right)\,, \tag{34}$$

where Ei(z) is the exponential integral function. We also need the the real space represenation obtained after inverse Fourier transformation,

$$\chi_{\|}^{\mathrm{3D}}(\omega,\mathbf{r})'' = \sqrt{\frac{2}{\pi}}\frac{1}{r}\int_0^\infty dqq\chi_{\|}^{\mathrm{3D}}(\omega,q)''\sin(qr)\,. \tag{35}$$

In order to perform the above integral we note that the imaginary part of the longitudinal susceptibility, given by Eq. (34), is peaked around $q = \sqrt{\omega/D}$ with the width of the peak $(1/\sqrt{\beta D})$ much smaller than its position in the regime we are working in $(\omega \gg T)$. For $\mathbf{r} = \mathbf{0}$, the integration over q can be then performed approximately and yields the following expression

$$\chi_{\|}^{\mathrm{3D}}(\omega,\mathbf{r}=\mathbf{0})'' = \frac{\sqrt{\pi}e^{-e^{-\beta\Delta_F}-3\beta\Delta_F/2}}{2\beta^2 D^3}\left(e^{e^{-\beta\Delta_F}+\beta\Delta_F/2}\right.$$
$$- e\sqrt{\pi}\sqrt{e^{\beta\Delta_F}-1} \tag{36}$$
$$\left.\times\ \mathrm{Erfc}(e^{-\beta\Delta_F/2}\sqrt{e^{\beta\Delta_F}-1})\right)\sqrt{\beta\omega}\,,$$

where Erfc(z) denotes the complementary error function. It is readily observed from the above expression that the longitudinal fluctuations are exponentially suppressed by the gap. Assuming that $\Delta_F \gg T$, we obtain the following simplified expression

$$\chi_{\|}^{\mathrm{3D}}(\omega,\mathbf{r}=\mathbf{0})'' = \frac{\sqrt{\pi} - e\pi\mathrm{Erfc}(1)}{2\beta^2 D^3}e^{-\beta\Delta_F}\sqrt{\beta\omega}\,. \tag{37}$$

We observe that, since $J(\omega) = \chi_{\|}(\omega,\mathbf{r})''$, the longitudinal noise of ferromagnet is—as the transverse one—subohmic [2].

Next we calculate the longitudinal fluctuations for the case of a quasi- one-dimensional ferromagnet $(\Delta_F \gg T)$ and obtain

$$\chi_{\|}^{\mathrm{1D}}(\omega,r=0)'' = \frac{1}{4\pi}\int_{-\infty}^{\infty}dk\int_{-\infty}^{\infty}dq\left(\frac{1}{e^{\beta(\Delta_F+Dk^2)}-1}\right.$$
$$\left. - \frac{1}{e^{\beta(\omega+\Delta_F+Dk^2)}-1}\right)\delta(\omega - Dq^2 - 2Dkq)$$
$$= \int_{-\infty}^{\infty}dk\frac{e^{-\beta Dk^2}}{1 - e^{-\beta\Delta_F} + \beta Dk^2}\frac{1}{D\sqrt{k^2+\omega/D}}$$
$$= \frac{\gamma}{D\sqrt{\beta\omega}}e^{-\beta\Delta_F}\,, \tag{38}$$

where γ is a numerical factor of order 1.

SCHRIEFFER-WOLFF TRANSFORMATION AND SPIN-SPIN COUPLING

Exchange coupling to the ferromagnet

The total Hamiltonian of the system reads

$$H = H_F + H_\sigma + A\sum_{\boldsymbol{i}}\left(\frac{1}{2}(\sigma_i^+ S_{\mathbf{r}_i}^- + \sigma_i^- S_{\mathbf{r}_i}^+) + \sigma_i^z S_{\mathbf{r}_i}^z\right)\,, \tag{39}$$

where we identify the main part as $H_0 = H_F + H_\sigma$ and the small perturbation as the exchange coupling $V = A\sum_{\boldsymbol{i}}\boldsymbol{\sigma}_i\cdot\boldsymbol{S}_{\boldsymbol{r}_i}$. The Hamiltonian of the ferromagnet reads $H_F = -J\sum_{\langle\boldsymbol{r},\boldsymbol{r}'\rangle}\boldsymbol{S}_{\boldsymbol{r}}\cdot\boldsymbol{S}_{\boldsymbol{r}'}$, while the Hamiltonian for the two distant qubits is $H_\sigma = \frac{\Delta}{2}\sum_{i=1,2}\sigma_i^x$.

The second order effective Hamiltonian [3] is given by $H_{\mathrm{eff}}^{(2)} = H_0 + U$, where

$$U = -\frac{i}{2}\lim_{\eta\to0^+}\int_0^\infty dte^{-\eta t}[V(t),V]\,, \tag{40}$$

where $V(t) = e^{iH_0t}Ve^{-iH_0t}$.

We have

$$\sigma_i^+(t) = \frac{1+\cos(\Delta t)}{2}\sigma_i^+ + \frac{1-\cos(\Delta t)}{2}\sigma_i^- - i\sin(\Delta t)\sigma_i^z\,, \tag{41}$$

and $\sigma_i^-(t) = \sigma_i^+(t)^\dagger$.

Recalling that the zz susceptibility can be neglected and that only the transverse susceptibility contributes, we obtain the following result from Eq. (40), $U = \lim\limits_{\eta\to0^+}\int_0^\infty dte^{-\eta t}\sum_{ij}U_{ij}$

$$U_{ij} = -\frac{iA^2}{8}\left([\sigma_i^-(t)S_{\mathbf{r}_i}^+(t),\sigma_j^+S_{\mathbf{r}_j}^-] + \mathrm{h.c.}\right)$$
$$= -\frac{iA^2}{8}\left(\sigma_i^-(t)\sigma_j^+[S_{\mathbf{r}_i}^+(t),S_{\mathbf{r}_j}^-] + \mathrm{h.c.}\right) \tag{42}$$

Finally, by rewriting $\cos(\Delta t) = \frac{e^{i\Delta t}+e^{-i\Delta t}}{2}$, $\sin(\Delta t) = \frac{e^{i\Delta t}-e^{-i\Delta t}}{2i}$, and using the definition of the real space transverse spin susceptibility

$$\chi_\perp(\omega,\mathbf{r}_i-\mathbf{r}_j) = -i\lim_{\eta\to0^+}\int_0^\infty dte^{(i\omega-\eta)t}[S_{\mathbf{r}_i}^+(t),S_{\mathbf{r}_j}^-]\,, \tag{43}$$

we obtain by inserting Eq. (41) into Eq. (42)

$$\begin{aligned} U =& \frac{A^2}{8} \sum_{ij} \left(\frac{\chi_\perp(0)}{2} + \frac{\chi_\perp(\Delta) + \chi_\perp(-\Delta)}{4} \right) \sigma_i^- \sigma_j^+ \\ &+ \frac{A^2}{8} \sum_{ij} \left(\frac{\chi_\perp(0)}{2} - \frac{\chi_\perp(\Delta) + \chi_\perp(-\Delta)}{4} \right) \sigma_i^+ \sigma_j^+ \\ &- \frac{A^2}{8} \sum_{ij} \frac{\chi_\perp(\Delta) - \chi_\perp(-\Delta)}{2} \sigma_i^z \sigma_j^+ + \text{h.c.} \end{aligned} \tag{44}$$

Since the decay length of the susceptibility $\chi(\omega, \mathbf{r})$ is large only close to the resonance, $\Delta_F \sim \Delta$, we can simplify the above equation by neglecting $\chi(-\Delta, \mathbf{r})$ and $\chi(0, \mathbf{r})$ in comparison to $\chi(\Delta, \mathbf{r})$ which is assumed to be close to the resonance. Within this approximation we arrive at Eq. (3) of the main text.

Dipolar coupling to the ferromagnet

The total Hamiltonian of the system reads

$$H = H_F + H_\sigma + H_I, \tag{45}$$

where the interaction between the spin-qubit and the ferromagnet, H_I, reads

$$H_I = \sum_{i,\mathbf{r}} \frac{\mu_0 \mu_B \mu}{4\pi r^3} \left(\boldsymbol{\sigma}_i \cdot \boldsymbol{S}_\mathbf{r} - \frac{3(\boldsymbol{\sigma}_i \cdot \mathbf{r})(\boldsymbol{S}_\mathbf{r} \cdot \mathbf{r})}{r^2} \right), \tag{46}$$

where μ is the magnetic moment of the ferromagnet, which is usually on the order of the Bohr magneton μ_B. After performing a second order SW transformation we obtain the correction to the uncoupled Hamiltonian

$$\begin{aligned} U =& - \lim_{\nu \to 0+} \frac{i}{2} \int_0^\infty e^{-\nu t} dt \frac{\mu_0^2 \mu_B^2 \mu^2}{16\pi^2 a^6} \int_V d\mathbf{r}' d\mathbf{r}'' \frac{1}{r'^3 r''^3} \times \\ & \left[\boldsymbol{\sigma}_1(t) \cdot \boldsymbol{S}_{\mathbf{r}'}(t) - \frac{3(\boldsymbol{\sigma}_1(t) \cdot \mathbf{r}')(\boldsymbol{S}_{\mathbf{r}'}(t) \cdot \mathbf{r}')}{r'^2}, \right. \\ & \left. \boldsymbol{\sigma}_2 \cdot \boldsymbol{S}_{\mathbf{r}''} - \frac{3(\boldsymbol{\sigma}_2 \cdot \mathbf{r}'')(\boldsymbol{S}_{\mathbf{r}''} \cdot \mathbf{r}'')}{r''^2} \right] + 1 \leftrightarrow 2, \end{aligned} \tag{47}$$

where $a = (V/N)^{1/3}$ is the lattice constant of the ferromagnet, This constant emerges in the above expression when going from the sum over the ferromagnetic spins to the integral over the ferromagnet volume. The above expression can be significantly simplified if a specific geometry of the ferromagnet is assumed. Namely, we assume a dog-bone shaped ferromagnet—two ferromagnetic discs joined by a thin ferromagnetic channel. We assume that the radius of the two discs is much smaller than the distance between their centers ($R_0 \ll L$). Within this assumption we can take for the susceptibility between two points at opposite discs the same as the 1D susceptibility given in Eq. (29). Now there are two independent axial symmetries under the rotations around the axes passing through the spin qubit and the adjacent center of the disc (we assume the z-axis to be parallel to these axes). Due to this symmetry only terms like $r'_+ r'_-$ and $r''_+ r''_-$ will give non-zero results upon integration over the discs. We also neglect the longitudinal susceptibility compared to the transverse one and arrive finally at the following expression

$$H_{\text{eff}} = H_\sigma + \frac{B^2}{32} \chi_\perp^{1\text{D}}(\Delta, L)(2\sigma_1^y \sigma_2^y - \sigma_1^z \sigma_2^x - \sigma_1^x \sigma_2^z), \tag{48}$$

where we retained only the on-resonance susceptibility, i.e., we neglected $\chi_\perp^{1\text{D}}(-\Delta)$ and $\chi_\perp^{1\text{D}}(0)$ in comparison to $\chi_\perp^{1\text{D}}(\Delta)$. The constant B in the above formula reads

$$B = \frac{\mu_0 \mu_B \mu}{2a^3} \int_{d_1}^{d_2} dz \int_0^{R_0} \rho d\rho \frac{1}{(z^2 + \rho^2)^{3/2}} \left(2 - \frac{3\rho^2}{z^2 + \rho^2} \right), \tag{49}$$

where $d_2 - d_1$ is the thickness of the discs, d_1 is the distance in z-direction from the spin qubit to the bottom of the adjacent disc. The above integral can be easily performed and yields the following result

$$B = \frac{\mu_0 \mu_B \mu}{2a^3} \left(\frac{d_2}{\sqrt{d_2^2 + R_0^2}} - \frac{d_1}{\sqrt{d_1^2 + R_0^2}} \right) \tag{50}$$

IMPLEMENTATION OF TWO-QUBIT GATES

Two qubits interacting via the ferromagnet evolve according to the Hamiltonian $H = H_{\text{eff}} + H_\sigma$, the sum of the qubit-qubit coupling and Zeeman term. These contributions, by and large, do not commute, making it difficult to use the evolution to implement standard entangling gates. Nevertheless, since H_σ acts only in the subspace spanned by $\{|+,+\rangle, |-,-\rangle\}$ and $\Delta \gg J_{12} = A^2 \chi_\perp(\Delta)/4$, we can neglect the effect of H_{eff} in this part of the space and approximate it by its projection in the space spanned by vectors $\{|+,-\rangle, |-,+\rangle\}$

$$H'_{\text{eff}} = J_{12}(\sigma_1^y \sigma_2^y + \sigma_1^z \sigma_2^z). \tag{51}$$

Within this approximation, the coupling in H'_{eff} and Zeeman terms now commute.

We consider the implementation of the iSWAP gate $U_{\text{iSWAP}} = e^{-i(\sigma_1^x \sigma_2^x + \sigma_1^y \sigma_2^y)3\pi/4}$, which can be used to implement the CNOT gate. The Hamiltonian H' already contains a $\sigma_1^y \sigma_2^y$ term, so implementation of the iSWAP gate requires only that the $\sigma_1^z \sigma_2^z$ term is transformed into $\sigma_1^x \sigma_2^x$ by appropriate local rotations. This is achieved with the following sequence

$$U_{\text{iSWAP}} = \mathcal{H}_1 \mathcal{H}_2 e^{iH_\sigma t} e^{-iH'_{\text{eff}} t} \mathcal{H}_1 \mathcal{H}_2, \tag{52}$$

where $t = 3\pi/(4J_{12})$ and $\mathcal{H}$ denotes the single qubit Hadamard rotation. When iSWAP is available, the CNOT gate can be constructed in the standard way [4]

$$U_{\text{CNOT}} = e^{-i\frac{\pi}{4}\sigma_1^z} e^{i\frac{\pi}{4}\sigma_2^x} e^{i\frac{\pi}{4}\sigma_2^z} U_{\text{iSWAP}} e^{-i\frac{\pi}{4}\sigma_1^x} U_{\text{iSWAP}} e^{i\frac{\pi}{4}\sigma_2^z}. \tag{53}$$

Since H'_{eff} is an approximation of H_{eff}, the above sequence will yield approximate CNOT, U'_{CNOT}, when used with the full Hamiltonian. The success of the sequences therefore depends on the fidelity of the gates, $F(U'_{\text{CNOT}})$. Ideally this would be defined using a minimization over all possible states of two qubits. However, to characterize the fidelity of an imperfect CNOT it is sufficient to consider the following four logical states of two qubits [5]: $|+,0\rangle, |+,1\rangle, |-,0\rangle$, and $|-,1\rangle$. These are product states which, when acted upon by a perfect CNOT, become the four maximally entangled Bell states $|\Phi^+\rangle, |\Psi^+\rangle, |\Phi^-\rangle$, and $|\Psi^-\rangle$, respectively. As such, the fidelity of an imperfect CNOT may be defined,

$$F(U'_{\text{CNOT}}) = \min_{i\in\{+,-\},j\in\{0,1\}} |\langle i,j| U^{\dagger}_{\text{CNOT}} U'_{\text{CNOT}} |i,j\rangle|^2. \tag{54}$$

The choice of basis used here ensures that $F(U'_{\text{CNOT}})$ gives a good characterization of the properties of U'_{CNOT} in comparison to a perfect CNOT, especially for the required task of generating entanglement. For realistic parameters, with the Zeeman terms two order of magnitude stronger than the qubit-qubit coupling, the above sequence yields fidelity for the CNOT gate of 99.976%.

To compare these values to the thresholds found in schemes for quantum computation, we must first note that imperfect CNOTs in these cases are usually modelled by the perfect implementation of the gate followed by depolarizing noise at a certain probability. It is known that such noisy CNOTs can be used for quantum computation in the surface code if the depolarizing probability is less than 1.1% [6]. This corresponds to a fidelity, according to the definition above, of 99.17%. The fidelities that may be achieved in the schemes proposed here are well above this value and hence, though they do not correspond to the same noise model, we can expect these gates to be equally suitable for fault-tolerant quantum computation.

DECOHERENCE

The two-qubit system dynamics can be described by the reduced density matrix $\rho_{\text{R}}(t) = \text{tr}\,(\rho(t))$, where ρ is the density matrix for the total system and the trace is taken over the degrees of freedom of the ferromagnet. The reduced density matrix $\rho_{\text{R}}(t)$ satisfies the Generalized Master Equation (GME) [2]

$$\dot{\rho}_{\text{R}}(t) = -i\,[H_\sigma, \rho_{\text{R}}(t)] + \int_0^t dt' \Sigma(t-t')\rho_{\text{R}}(t')\,. \tag{55}$$

The self-energy $\Sigma(t-t')$ is a super-operator acting on $\rho_{\text{R}}(t)$. We assume that at the initial time $t = 0$ the system of the qubit spins and the system of the ferromagnet are decoupled, and the ferromagnet is in thermal equilibrium, $\rho(0) = \rho_{\text{R}}(0) \otimes \rho^{eq}$, where $\rho^{eq} = e^{-H_F/k_BT}/\text{tr}\left(e^{-H_F/k_BT}\right)$.

We calculate the self-energy $\Sigma(t-t')$ of Eq. (55) in Born approximation. We assume that the reduced density matrix $\rho_{\text{R}}(t)$ varies slowly compared to the time scale of the ferromagnet, $\hbar/J$, and thus we employ the Markov approximation in Eq.(55). The result of this reads

$$\dot{\rho}_{\text{R}} = -i[H_\sigma, \rho_{\text{R}}] + \left(\sum_{p=1,2} \mathcal{D}_p + \mathcal{D}_{\text{corr}}\right)\rho_{\text{R}}\,, \tag{56}$$

where $\mathcal{D}_p$ ($p = 1,2$) describes uncorrelated noise (i.e. Korringa relaxation), and $\mathcal{D}_{\text{corr}}$ describes correlated noise between the two qubits under the consideration. We ignore the correlated noise in what follows and set $\mathcal{D}_{\text{corr}} = 0$ in Eq. (56). The reason for such a treatment is that we obtain the decoherence times due to uncorrelated noise to be much bigger than all the other time scales in the system, and the inclusion of the correlated noise [7] cannot alter this statement [8]. We have ignored the Stark and Lamb shift since these second order corrections are much smaller than the first order one we already included, see Eq. (2) of the main text. Therefore, in the main text we study decoherence due to coupling a single qubit to the ferromagnet.

EXACT TREATMENT

As noted earlier, the transversal noise of the ferromagnet is gapped and it does not contribute to decoherence in the lowest order. This motivate us to study a model where we have only longitudinal coupling to the ferromagnet. After making use of harmonic approximation for the ferromagnet we arrive at the Hamiltonian that can be exactly solved since it can be related to the exactly solvable 'independent Boson problem' [9]. Instead of Eq. (1) of the main text, we have a simplified Hamiltonian of the system

$$H = H_0 + \sigma_z \otimes V\,, \tag{57}$$

with $H_0 = \sum_{\mathbf{q}} \hbar\omega_{\mathbf{q}} a^{\dagger}_{\mathbf{q}} a_{\mathbf{q}} + \varepsilon\sigma_z$ and $V = \sum_{\mathbf{q}} \sqrt{S}(a^{\dagger}_{\mathbf{q}} + a_{\mathbf{q}})$.

Since σ_z commutes with the total Hamiltonian, only dephasing can occur in the system. In order to study dephasing we have to calculate the following quantity [10]

$$\begin{aligned}\langle\sigma_-(t)\rangle = e^{i\varepsilon t/\hbar}\langle\sigma_-(0)\rangle\times \\ \times \left\langle \tilde{T}\text{exp}\left(\frac{i}{2}\int_0^t V dt'\right) T\text{exp}\left(\frac{i}{2}\int_0^t V dt'\right)\right\rangle.\end{aligned} \tag{58}$$

The average in the above formula can be calculated using a cluster expansion [11], and since the perturbation V is linear in the bosonic operators, only the second order cluster contributes. Therefore, the final exact result for the time-evolution of $\sigma_-(t)$ reads

$$\langle\sigma_-(t)\rangle = e^{i\varepsilon t/\hbar}\langle\sigma_-(0)\rangle e^{-\frac{1}{2}\int_0^t\int_0^t S(t_2-t_1)dt_1dt_2}\,, \tag{59}$$

where $S(t) = \langle [V(t), V(0)]_+ \rangle$. Furthermore, we can express this result in terms of the spectral function $J(\omega) = \tanh(\beta\omega/2) S(\omega)$

$$\langle \sigma_-(t) \rangle = e^{i\varepsilon t/\hbar} \langle \sigma_-(0) \rangle \times \qquad (60)$$
$$\times \exp\left(-\frac{1}{2} \int \frac{d\omega}{2\pi} J(\omega) \coth(\beta\omega/2) \frac{\sin^2(\omega t/2)}{(\omega/2)^2} \right) .$$

Note that the above formula is of the exactly same form as the one for a *classical* Gaussian noise [12]. Now we apply this formula to the case of the ferromagnetic bath.

At zero temperature, we obtain from Eq. (60) the dephasing behavior described by the evolution $\langle \sigma_-(t) \rangle \sim e^{-\frac{\tilde{\omega}_s \sqrt{t}}{\sqrt{2\pi\omega_s}} + i\varepsilon t}$. In stark contrast to this, a naive use of the Born-Markov approximation leads to the incorrect conclusion that the dephasing is absent [2]. However, we note that the latter approximation is no longer self-consistent in this regime since the perturbation (coupling to the ferromagnetic bath) becomes bigger than the system energy scales (which vanishes for zero splitting). Since the longitudinal noise of the ferromagnet is completely absent at $T = 0$, we next analyse dephasing for non-zero temperature. The Born-Markov approximation again leads to divergent result at non-zero temperature, which again is spurious. The exact solution for $T \neq 0$, and for long times $t \gg \hbar/T$ leads to the well-behaved dynamics of the form

$$\langle \sigma_-(t) \rangle \sim e^{-16A^2 T^{5/2} t^{3/2}/D^3 + i\varepsilon t} . \qquad (61)$$

Therefore, for zero splitting of the qubit (or $\Delta \ll A$), the dephasing is much stronger then in the case when the splitting is present. This was the reason for including the splitting of the qubit.

[1] W. Nolting and A. Ramakanth, *Quantum Theory of Magnetism* (Springer, 2009).

[2] D. P. DiVincenzo and D. Loss, Phys. Rev. B **71**, 035318 (2005).

[3] S. Bravyi, D. DiVincenzo, and D. Loss, Ann. Phys. **326**, 2793 (2011).

[4] T. Tanamoto, K. Maruyama, Y. X. Liu, X. Hu, and F. Nori, Phys. Rev. A **78**, 062313 (2008).

[5] L. Trifunovic, O. Dial, M. Trif, J. R. Wootton, R. Abebe, A. Yacoby, and D. Loss, Phys. Rev. X **2**, 011006 (2012).

[6] D. S. Wang, A. G. Fowler, and L. C. L. Hollenberg, Phys. Rev. A **83**, 020302 (2011).

[7] Y. Rikitake and H. Imamura, Phys. Rev. B **72**, 033308 (2005).

[8] The uncorrelated noise is related to the quantity $\chi_\parallel(\omega, \mathbf{r} = \mathbf{0})''$ and the correlated one is given by the same quantity but taken at the separation between the two qubits, $\chi_\parallel(\omega, \mathbf{r})'' \leq \chi_\parallel(\omega, \mathbf{r} = \mathbf{0})''$. Therefore the correlated noise cannot exceed the uncorrelated one.

[9] G. D. Mahan, *Many Particle Physics*, 3rd ed. (Springer, 2000).

[10] Y. Makhlin and A. Shnirman, Phys. Rev. Lett. **92**, 178301 (2004).

[11] A. A. Abrikosov, L. P. Gorkov, and I. E. Dzyaloshinski, *Methods of Quantum Field Theory in Statistical Physics* (Dover, 1975).

[12] Y. Makhlin, G. Schön, and A. Shnirman, Chem. Phys. **296**, 315 (2004).